Science Press

ARTICLE

Numerical Analysis on Die Wear and Macrostructure Delamination Characteristics of Titanium Alloy Frame in Hot Forging

Teng Haihao[1],   Xia Yufeng[1,2],   Yu Yingyan[1,2],   Yin Hui[3]

[1] College of Materials Science and Engineering, Chongqing University, Chongqing 400045, China; [2] Chongqing Key Laboratory of Advanced Mold Intelligent Manufacturing, Chongqing University, Chongqing 400044, China; [3] China National Erzhong Group Deyang Wanhang Die Forging Co., Ltd, Deyang 618013, China

Abstract: The microstructure of TC18 titanium alloy die forging shows delamination. The brighter microstructure has lower performance and is often called cold die microstructure (CDM). Decreasing the cooling rate can hinder the generation of CDM, but it may also aggravate the die wear. The balance relation between microstructure delamination of TC18 frame forging and the die wear in different parameters was studied by simulation and experiment. The programs to predict the CDM and wear depth were built and realized by secondary development. Continuous forging production process was simulated by DEFORM software and the characteristics of CDM and wear were researched. The balance relationship between the die wear and the CDM content in different parameters was discussed by the response surface method and the optimal parameters. Results show that the preheating temperature of die plays a dominant role in the variation of the wear depth. The most influential factor of CDM content is the contact condition. Applying glass fiber can reduce the CDM content without increasing the wear depth.

Key words: die wear; titanium forging; macrostructure delamination; secondary development

Due to good hardenability, weldability and excellent damage tolerance, TC18 titanium is widely used in the aircraft structural parts[1]. Usually, die forging is used to form TC18 parts of aircraft with complex shape, such as landing gear and frame. As shown in Fig. 1, there is apparent macrostructure
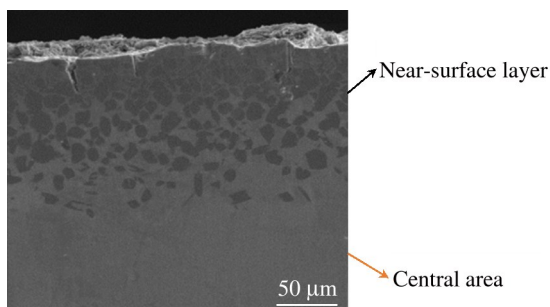

Fig.1   Schematic of the TC18 forging section

delamination in TC18 forgings in production, because of the nonuniformity of temperature and deformation distribution. The near-surface layer for TC18 forging is brighter than the central area with coarse β grain. The bright microstructure has worse performance than the center, reducing the material utilization rate and even destroying the forging streamline. Because the bright microstructure is near the die, it is called the cold die microstructure (CDM).

Some studies have been performed on the CDM. Ahmed[2] et al studied mechanical properties of CDM. Chen[3] et al summarized the mechanism and formation conditions of CDM based on thermal simulation experiments. Based on their conclusions, increasing the preheating temperature can decrease the CDM content but it may also induce die softening and enlarge the wear depth[4]. Meanwhile, heat transformation can also affect the field distribution and the CDM generation. The CDM distribution and die wear have a

complex relationship, and research on their balance is greatly significant for both forging quality controlling and die life increasing. However, all aforementioned studies have ignored the problem.

Therefore, the current study used the finite element model (FEM) to accurately simulate the continuous production process of titanium alloy forging. The programming for CDM and die wear depth prediction of the related mathematical model was realized by the secondary developed interface provided by DEFORM. The balance relation between die wear and CDM percent of titanium forging was studied, and the process parameters were optimized for the balance through

$$
\begin{cases}
\sigma = \dfrac{1}{\alpha(\varepsilon)} a\sinh\left\{\left[\dfrac{\dot{\varepsilon}}{A(\varepsilon)}\exp\dfrac{Q(\varepsilon)}{RT}\right]^{\frac{1}{n(\varepsilon)}}\right\} \\[4mm]
\begin{Bmatrix} a \\ n \\ Q \\ \ln A \end{Bmatrix} = \begin{pmatrix}
0.0072 & 4.916 & 318.763 & 32.029 \\
-0.00209 & -43.931 & -346.236 & 1.417 \\
0.505 & 690.976 & 13451.5 & 421.825 \\
-5.973 & -5916.37 & -237283 & -13037.22 \\
35.987 & 27987.11 & 1712540 & 10795511 \\
-104.07 & -67878.47 & -5521260 & -370079.2 \\
114.560 & 65587.323 & 6582240 & 457675.82
\end{pmatrix}\begin{Bmatrix} \varepsilon_1 \\ \varepsilon_2 \\ \varepsilon_3 \\ \varepsilon_4 \\ \varepsilon_5 \\ \varepsilon_6 \end{Bmatrix}
\end{cases}
\tag{1}
$$

Some thermo-physical properties (such as density and specific heat) of the two metals in simulations were calculated by the thermodynamic calculation. The phase composition of the two alloys were firstly predicted under different temperature equilibrium conditions[6]. Then according to the phase composition and properties of each phase, the overall properties of the alloy can be calculated by the mixing law as shown in Eq.(2).

$$p = \sum x_i p_i Q_i \tag{2}$$

where x_i is the mass fraction of the pivot element, p_i means the thermal properties of pure components, and Q_i is the component interaction coefficient. All material parameters can be obtained by invoking the thermodynamic database.

The Jmatpro software was used to integrate the above models. Through continuous optimization, the software can rapidly predict the properties of metal materials. The prediction accuracy has been widely verified. The thermo-physical properties of two alloys were calculated for further simulations, as shown in Table 3.

1.2 Wear and CDM prediction models

1.2.1 Wear model

The Archard-type wear model is extensively adopted for wear depth prediction, as shown in Eq.(3)[7]:

Table 1 Chemical composition of TC18 alloy (wt%)

Al	Mo	V	Cr	Fe	C	O	N	Ti
5.12	5.14	5.06	0.93	0.98	0.01	0.15	0.02	Bal.

Table 2 Chemical composition of 5CrNiMo steel (wt%)

C	Mn	Si	S	P	Cr	Ni	Mo	Fe
0.55	0.70	0.31	0.02	0.02	0.71	1.62	0.25	Bal.

the response surface. The research provides essential guidance for decreasing wear failure and die manufacture cost.

1 Simulation Approach

1.1 Basic material parameters

TC18 titanium alloy was selected as the material for the frame. Its flow stress model was taken directly from the research results of Lei[5], as shown in Eq.(1), and the basic parameters of TC18 are shown in Table 1. 5CrNiMo die steel was used as the die material, and the chemical composition of which is shown in Table 2.

$$W = K\frac{LP}{H} \tag{3}$$

where W denotes the wear depth, K means the wear coefficient, H is the die hardness, L is the relative sliding distance, and P is the contact pressure between the workpiece and die.

Owing to the fact that H is temperature-dependent, the model considers it as a constant[6], so it will bring specific errors in hot forging operations. Therefore, Eq.(3) can be changed to Eq.(4)[8].

$$W = \int_0^t k\frac{LP}{H(T)}\,\mathrm{d}t \tag{4}$$

where $H(T)$ is the function of die hardness and t is sliding time. For 5CrNiMo steel, $H(T)$ can be obtained by Eq.(5).

$$H(T) = 45 - \left(\frac{T}{500}\right)^9 \tag{5}$$

During forging processes, the relative sliding velocity, contact pressure and temperature fields vary with the position and time. Hence, Eq.(4) can be further modified to Eq.(6)

$$W = \int_0^t k\frac{p_{ij}V_{ij}}{H(T)}\,\mathrm{d}t \tag{6}$$

where V_{ij} is relative sliding velocity and p_{ij} is contact pressure. The Archard-type wear model was verified in pre-production.

1.2.2 CDM prediction model

From the research of Chen et al[3], the criterion of the CDM

Table 3 Thermo-physical properties of TC18 at 850 °C and 5CrNiMo steel at 400 °C

Property	TC18	5CrNiMo
Density/g·cm^{-3}	4.61	7.82
Thermal conductivity/W·(m·K)$^{-1}$	21.93	20.9
Specific heat/J·(g·K)$^{-1}$	0.63	0.54

can be deduced, as shown in Eq.(7).

$$\varepsilon_c = 4.3 \times 10^7 \exp(-T/42.4) + 0.2 \qquad (7)$$

If the strain is higher than ε_c, there is net basket microstructure. Otherwise, it is CDM.

1.2.3 Secondary development of DEFORM

The DEFORM software provides several connectors for secondary development of preprocess and post-process[10]. In this work, the custom subroutine is compiled in the pre-processing stage, and the wear model of 5CrNiMo steel is written into the die-wear script (USRWEAR). Fig.2a presents the schematic of the pre-processing secondary development. In the post-processing stage, the criterion and distribution model of the CDM are compiled into the script file (pstusr.f) and linked to the dynamic link library file (USR_DEF_PST3. dll). The display of custom variables is realized by calling the library on the post-processing interface. Fig. 2b shows the schematic of the post-processing secondary development.

1.3 Validation for the two models

The modified mold wear model was integrated into DEFORM software for wear prediction, and the prediction accuracy was verified in the previous research. In this section, the prediction accuracy of Eq. (7) will be tested by non-isothermal thermal compression tests. The TC18 titanium alloy was wire-cut into rods with dimensions of 40 mm×50 mm. A resistance furnace was used to heat the billet to 890 °C

and the titanium alloy was held for 40 min to undergo a complete β transition. Then, the titanium alloy was quickly transferred to the hydraulic press, and the transfer time was about 15 s. The upsetting forming of titanium alloy with 40% in deformation was conducted at a forming speed of 5 mm/s. The titanium alloy sample after forming was cut for macroscopic detection, and the depth of CDM layer was measured. At the same time, DEFORM software was used to simulate the forming process and to predict the CDM layer depth of titanium alloy after forming.

Fig.3 shows the comparison of simulation and forging test results. The results show that due to the friction and temperature gradient, the deformation of titanium alloy in different regions during the upsetting process is very different, and the lantern shape is formed. The area where the titanium alloy is in contact with the mold produces CDM. The thickness of CDM predicted by FEM is about 6 mm, which is close to the experimental value. The secondary development of DEFORM software can be used to predict CDM depth of TC18 titanium alloy.

1.4 FEM of titanium alloy frame

The forging in this case is a connection frame of aircraft, and its shape is shown in Fig.4. The dimensions are 862 mm× 633 mm×221 mm and it weighs 93.8 kg. The frame's projective area is 0.34 m^2. Because of the large geometry and
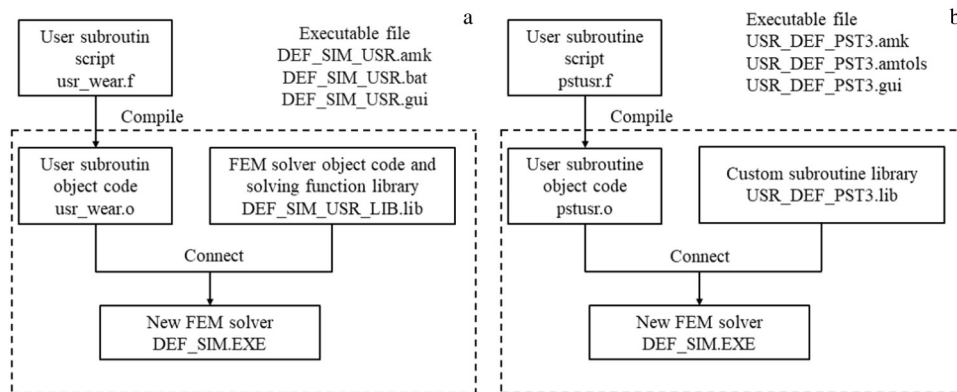

Fig.2   Schematic diagrams of secondary development: (a) pre-process and (b) post-process
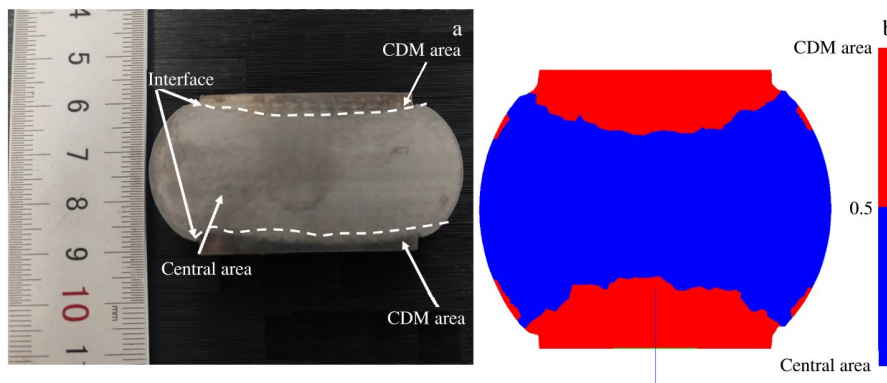

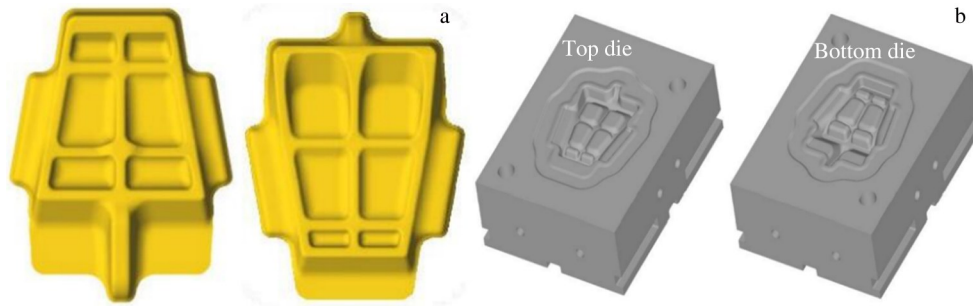Fig.3   Comparison of forging test (a) and simulation (b) results

Fig.4　Schemes of forging (a) and dies (b)

projective area, it is easy to transfer heat and to generate the CDM. Besides, the forging is symmetrical in the width direction. To simplify FEM model, 1/2 model was used in simulation.

The simulation scheme is shown in Fig. 5. Mesh is generated automatically by the software, and the number of workpiece elements and die elements is 250 000 and 100 000, respectively.

(1) Heating and transformation

The α/β phase transition temperature of TC18 alloy is about 865 °C. Before forming, it is usually heated to (β_T−5, β_T+ 30 °C)[11–13]. Due to red hardness, the die will be heated to 300– 400 °C. From heating to forming, alloys need some time to transport, decreasing surface temperature and generating the CDM. Therefore, the process cannot be ignored. According to statistics, it takes about 1800 and 60 s for the die and billet to transport, respectively. Compared to bare metal (Fig. 6a), a glass fiber (Fig. 6b) is often covered on the metal surface for thermal insulation. The heat transfer coefficient with air in various conditions is measured and shown in Fig. 6c. It is

worth noting that the glass fiber material will also increase the friction and forming loads. The influence of heat preservation on CDM and wear also needs to be studied.

(2) Forming

Parameters of forming are shown in Table 4. The hot forging process is assumed as follows[14–16]. Firstly, consider the die as rigid body and neglect its deformation. Secondly, the elastic deformation during formation is very slight so it is negligible, and thus the billet is set as the plastic body. Thirdly, the friction type is shear friction. The shear friction model is defined as f_s=mk, where f_s is the frictional stress, m is the coefficient of friction, and k is the shear yield stress.

(3) Die cooling

Die cooling has a great significance in continuous production. In production, high-pressure air is used to treat the die cavity for cooling and oxide scale removal. This process lasts about 2 s. And the transfer coefficient is affected by the concentration of water-based graphite, vaporization phase transition of water droplets and convection velocity, and its empirical value is 8 N·s⁻¹·mm⁻¹·°C⁻¹[17].
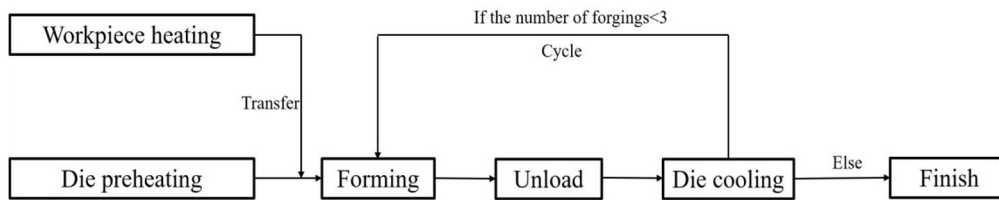

Fig.5　Scheme of the simulation

Fig.6　Bare metal (a), metal with glass fiber (b), and heat transfer coefficient (c)

Table 4　Parameters for forming simulation

Parameter	Value
Top die speed/mm·s^{-1}	5 (load) 15 (unload)
Environment temperature/°C	20
Heat transfer coefficient between billet dies/N·s^{-1}·mm^{-1}·°C^{-1}	7.5 (bare metal with water-based graphite) 1 (metal with glass fiber and lubricant) 0.8 (metal with new glass fiber)
Coefficient of friction	0.23 (bare metal with water-based graphite) 0.35 (metal with glass fiber and lubricant) 0.45 (metal with new glass fiber)
Increment/mm	1

2　Results and Discussion

2.1　Model validation

The hot forging experiment was conducted under 800 MN forging pressure. Fig. 7 shows the comparison between the forging experiment and simulation. The result shows a good agreement, suggesting that the simulation can well represent the metal deformation and die behavior in frame forging operation. Besides, the depth of the CDM is about 15 mm which is consistent with the actual situation.

Through further analyzing the wear distribution, it is found that the most severe position is the flash groove. The most important reason for that is die-softening. In production, the temperature rises most rapidly in the flash groove, causing the decrease in hardness to the minimum and the most serious wear, as shown in Fig. 8a and 8b. Moreover, as shown in Fig. 8c and 8d, the hindering effect of the flash groove will also enhance the relative sliding velocity and stress concentration and result in more severe die wear.

Fig. 9 shows the distribution of temperature, strain and the CDM. The CDM distribution is similar to the temperature field. For the inner metal, with the generation of deformation heat in forging, the temperature rises and the thermal conductivity decreases, making it difficult to transfer heat. The higher the temperature, the more significant the deformation, and sufficient dynamic recrystallization causes
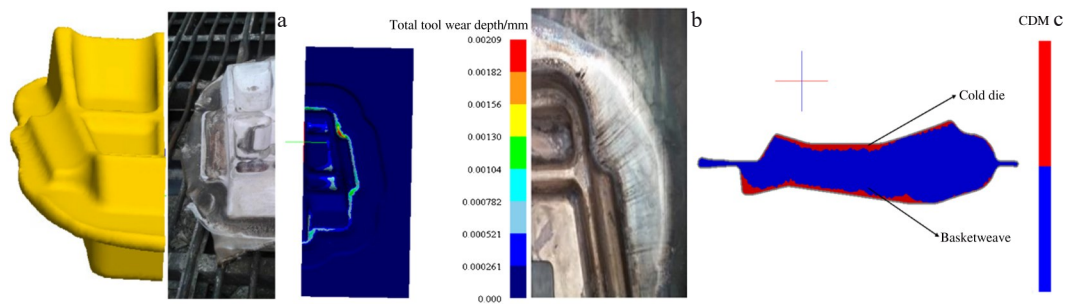

Fig.7　Comparison between forging experiment and simulation: (a) forging shape, (b) wear distribution, and (c) macrostructure delamination of forging
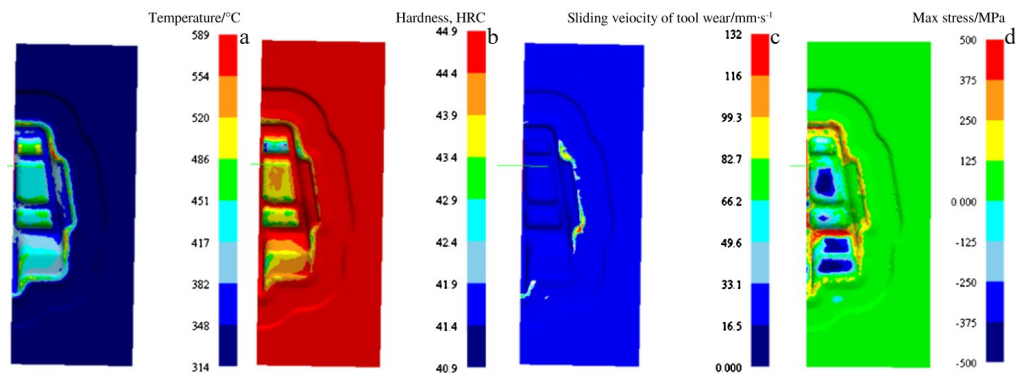

Fig.8　Temperature (a), hardness (b), sliding velocity (c), and max principal stress (d) of forging die
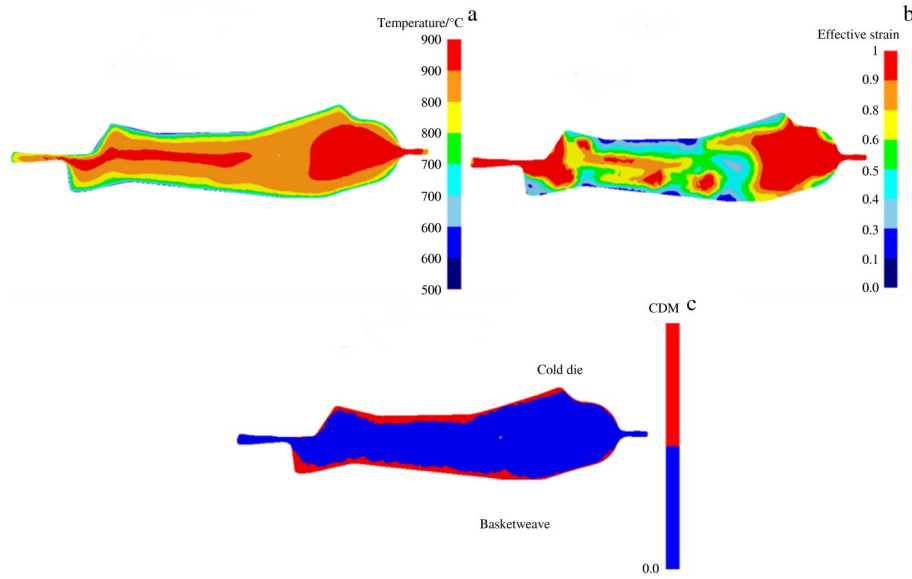
Fig.9   Temperature field (a), strain field (b), and macrostructure delamination (c) of forging

the α phase to precipitate in flake form during cooling[18–20]. Within the original grain, the β transformation structure will present different clusters after forging and annealing[21–22]. There are many approximately lamellar-parallel precipitated α phases in the same cluster. Many clusters interlace and weave into the basketweave microstructure. The part in contact with the die undergoes intense heat exchange due to temperature difference. If the cooling rate exceeds 1 °C/s, the α phase will precipitate in an equiaxed state[2]. Meanwhile, the precipitated α phase in the grain boundary is easier to nucleate and grow than the intracrystalline α phase since the solute atoms at the grain boundary diffuse more easily[23]. Under the effect of low strain and insufficient dynamic recrystallization, the surface metal will finally change to continuous α phase at grain boundaries combined with minor isometric α phase and lamellar secondary intercrystalline α phase, which is the CDM. During the forging of the frame, it is difficult for metal to flow at the rib, where the CDM is the most easily generated. How to optimize the parameters to reduce the CDM percent and wear depth without changing the die structure will be discussed next.

2.2 Process optimization

Based on the above analysis, it can be concluded that the CDM distribution and die wear are mainly determined by

temperature. However, the temperature field is also influenced by a set of process conditions: die-preheating temperature, forging temperature and contacting conditions. Thus, a multi-objective optimization design for frame forging is necessary to minimize the CDM percent and wear depth.

2.2.1   Experimental design and RSM modeling

In the multi-objective optimization design, the titanium preheating temperature x_1, die preheating temperature x_2 and contact conditions x_3 were adopted as design variables, and the CDM percent of forging maximum section y_1 and the wear depth y_2 were selected as response variables. The experimental design was carried out by the Box-Behnken-design (BBD) approach. Table 5 and Table 6 present the parameter levels and experimental results with 15 groups, respectively.

RSM is a collection of mathematical and statistical methods for investigating and analyzing the influences of the interaction of multiple variables on the optimization

Table 5   Parameters for forming simulation of the RSM

Level	x_1/°C	x_2/°C	x_3
−1	870	300	−1 (bared)
0	880	350	0 (glass fiber)
1	890	400	1 (new glass fiber)

Table 6   Experiment design and calculation results of the RSM

Scheme	x_1/°C	x_2/°C	x_3	y_1	y_2
1	870	300	0	0.300 388 6	0.002 574
2	880	350	0	0.314 923 825	0.002 018 25
3	870	350	−1	0.300 763 075	0.001 99
…	…	…	…	…	…
13	880	350	0	0.314 923 825	0.002 018 25
14	880	300	−1	0.309 965 1	0.002 3
15	890	400	0	0.292 125 9	0.002 09

objectives[24–25]. As RSM has significant advantages of reliability and continuity, it has been extensively applied in industrial production. Generally, a second-order polynomial response surface model is used, as shown in Eq.(8)[26]:

$$y = A_0 + \sum_{i=1}^{n} A_i x_i + \sum_{i=1}^{n} A_{ii} x_i^2 + \sum_{j=2}^{n} \sum_{i=1}^{j-1} A_{ij} x_i x_j \quad (8)$$

where y and x represent the response variables and design variables, respectively; A_0, A_i, A_{ii} and A_{ij} are the regression coefficients; n is the number of design variables.

The polynomial regression analysis of experimental results in Table 4 is carried out by the least square method, and then it is substituted into Eq. (8). The CDM percent of forging maximum section y_1 and wear depth y_2 can be obtained as follows:

$$y_1 = -112.6937 + 0.25891x_1 - 0.00546x_2 - 0.22395x_3$$
$$+ 0.00000866x_1x_2 + 0.000258x_1x_3 - 0.00004x_2x_3$$
$$- 0.000148x_1^2 - 0.0000032x_2^2 - 0.01104x_3^2 \quad (9)$$

$$y_2 = -0.4391 + 0.0011x_1 - 0.0003x_2 + 0.01435x_3$$
$$+ 0.00000035x_1x_2 - 0.00001625x_1x_3 - 0.0000008x_2x_3$$
$$- 0.00000074x_1^2 + 0.0000001194x_2^2 + 0.0000835x_3^2$$
$$(10)$$

2.2.2 Analysis of RSM

To verify the reliability of the RSM model, analysis of variance (ANOVA) was applied. The results of two models are obtained and shown in Table 7. F is homogeneity of variance test value by F-test, and P is the probability value. If the value of $P > F$ is less than 0.05, it means that the optimization target model has significant correlation. When the value of $P > F$ is less than 0.01, it indicates a highly significant correlation. The results show that the F values of the two quadratic models are 12.35 and 5.21, and the values of $P_{rob} > F$ are all less than 0.05, so the models are appropriate with 95% in confidence level.

In addition, four statistical factors, including the R^2 (coefficient of determination), Adj. R^2 (adjusted coefficient of determination), Pred. R^2 (predicted coefficient of determination) and adequate precision were also used to further test the fitting accuracy and prediction capacity of the responses. The statistical index values for both models are shown in Table 8, proving the accuracy of the RSM model. It can be seen that the values of R^2 and Adj. R^2 for both responses are close to 1, i. e., the response surface models are acceptable with high fitting accuracy. The differences of Adj. R^2 and Pred. R^2 for both models are smaller than 0.2, which indicates that the prediction accuracy is better. Furthermore, the resolution of the models is high, as adequate precision is greater than 4.

The interaction between parameters and responses can be shown by 3D surface plot developed by Design-Expert 10. Fig. 10 shows the surface plot of the CDM content of forging maximum section with the change of the titanium alloy

Table 7 Analysis of variance for each response

Response	Sum of squares	DF	Mean square	F value	$P_{rob} > F$
y_1	2.63×10^{-3}	9	0.000 293	12.35	0.001 6
y_2	3.581×10^{-7}	12	2.98×10^{-8}	5.21	<0.000 1

Table 8 Statistical factors for both responses

Response	R^2	Adj. R^2	Pred. R^2	Adequate precision
y_1	0.9408	0.9146	0.7169	9.636
y_2	0.9041	0.8937	0.7791	7.358

preheating temperature, die preheating temperature and contacting conditions, the interaction of which causes a significant bending of the response surface, demonstrating that the CDM content is significantly affected by the interaction of the three parameters. Among them, the contacting condition has the most significant effect on the CDM content and it is necessary to select appropriate insulation materials in forging. Besides, it is worth noting that the CDM content is not positively correlated with the preheating temperature. That is mainly because of the deformation heat. The deformation-heat in forging can be calculated by Eq.(11)[27]:

$$\Delta T = \frac{0.95\eta \int \sigma d\varepsilon}{\rho C_p} \quad (11)$$

where σ is the flow stress (MPa), ε is the strain, and η is the adiabatic correction factor which can be calculated by Eq.(12)[27]:

$$\eta = \begin{cases} 0 & \dot{\varepsilon} \leq 0.001 \text{ s}^{-1} \\ 0.316 \lg \dot{\varepsilon} + 0.95 & 0.001 \text{ s}^{-1} < \dot{\varepsilon} < 1 \text{ s}^{-1} \\ 0.95 & \dot{\varepsilon} \geq 1 \text{ s}^{-1} \end{cases} \quad (12)$$

According to Eq.(11) and Eq.(12), more deformation heat will be consumed at a lower temperature. Further, to study its influence on CDM content, the processes at different die temperatures with the same forging temperature and contact conditions were simulated. The results are shown in Fig. 11. Due to the deformation heat, the plasticity of metals is enhanced and the percent of low strain range is lessened, which promotes dynamic recrystallization and the formation of basketweave microstructure. Besides, the existence of deformation heat reduces the cooling rate of the surface. The α phase precipitates in flakes, which will hinder the generation of CDM. In addition, the low temperature on the forging surface reduces the thermal conductivity of alloy. An insulating layer forms, which can also reduce the cooling rate to a certain extent and thus suppress the generation of CDM.

Fig. 12 shows the relationship between the wear depth and the parameters. Unlike the CDM content, die wear is mainly affected by preheating temperature. The corrected Archard model shows that compared with the interface pressure and sliding speed, the hardness change significantly impacts wear. The hardness is mainly changed with the die temperature, which can be predicted by Eq.(13)[28]:

$$T_D(0,t) = 1/(1 + \frac{\lambda_2}{\lambda_1} \sqrt{\frac{\alpha_2}{\alpha_1}}) (T_{10} - T_{20}) + \frac{\mu p v}{\lambda_2} \sqrt{\alpha_{2t}} \quad (13)$$

where λ is the thermal conductivity (W·m^{-1}·°C^{-1}), μ is the friction coefficient, α is thermal diffusivity, t is the relative sliding time, and T_{10} and T_{20} and are the preheating temperature of the billet and die, respectively. In forging, the sliding time is
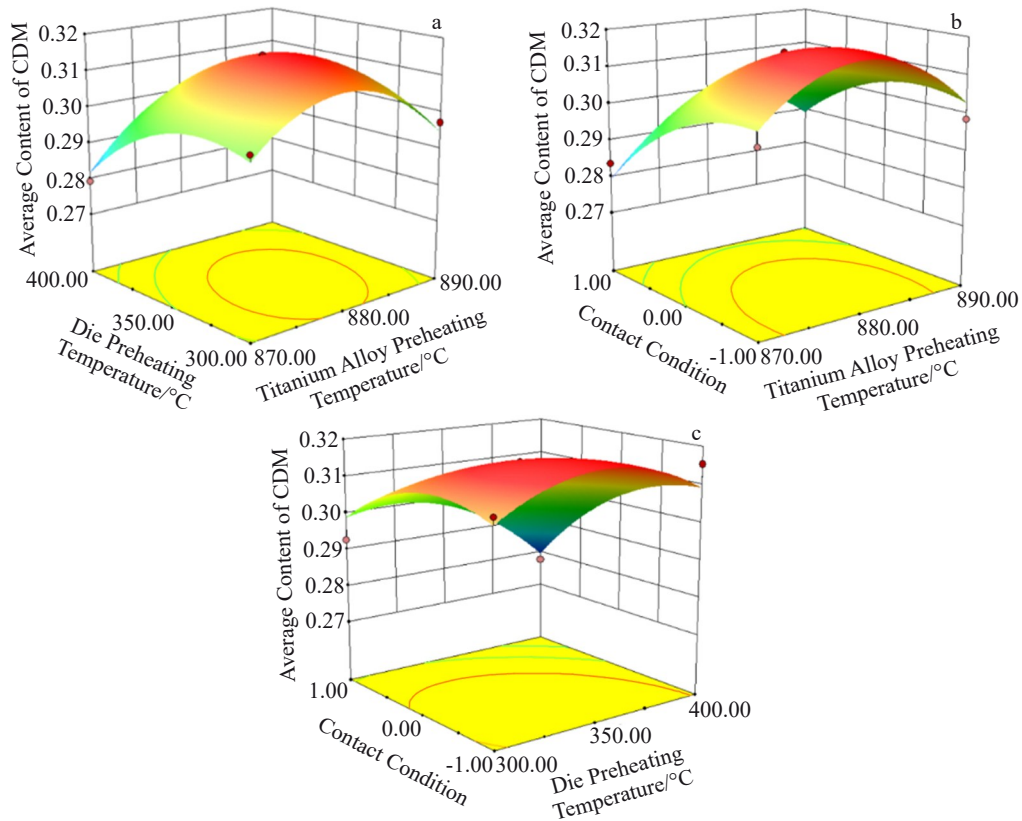
Fig.10   3D surface plots of average CDM content in different interaction conditions: (a) different die and titanium alloy preheating temperatures, (b) different titanium alloy preheating temperatures and contacting conditions, and (c) different die preheating temperatures and contacting conditions
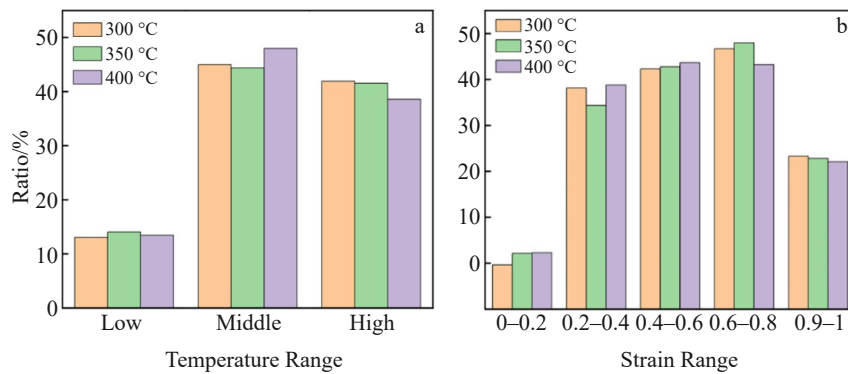

Fig.11   Ratio of temperature range (a) and strain range (b) at different die temperatures

short, so the degree of friction heat generation is far less than that of heat transfer. Compared with the preheating temperature of the die, the heating temperature of the alloy has a smaller range. Therefore, the service temperature of the die is mainly determined by the preheating temperature. Furthermore, applying glass fiber has little effect on wear depth even though it will increase the friction and load. Heat insulation of glass fiber hinders the temperature rise and softening of the die, which will lessen the wear depth. For this frame die, a reasonable temperature range of die (350–380 °C) is determined to weaken the wear.

2.2.3   Multi-objective optimization

The objective is the minimization of the CDM content and wear depth. The empirical relationships between design variables and responses from the RSM analysis are used as functional equations. The objective function and the limit of decision variables are shown as follows:

$$\begin{cases} \text{Minimize}\, f(x) = \{y_1(x_i), y_2(x_i)\} \\ x_1 \in [870, 890]\,(°C) \\ x_2 \in [300, 400]\,(°C) \\ x_3 = \text{INT}[-1, 1] \end{cases} \quad (14)$$
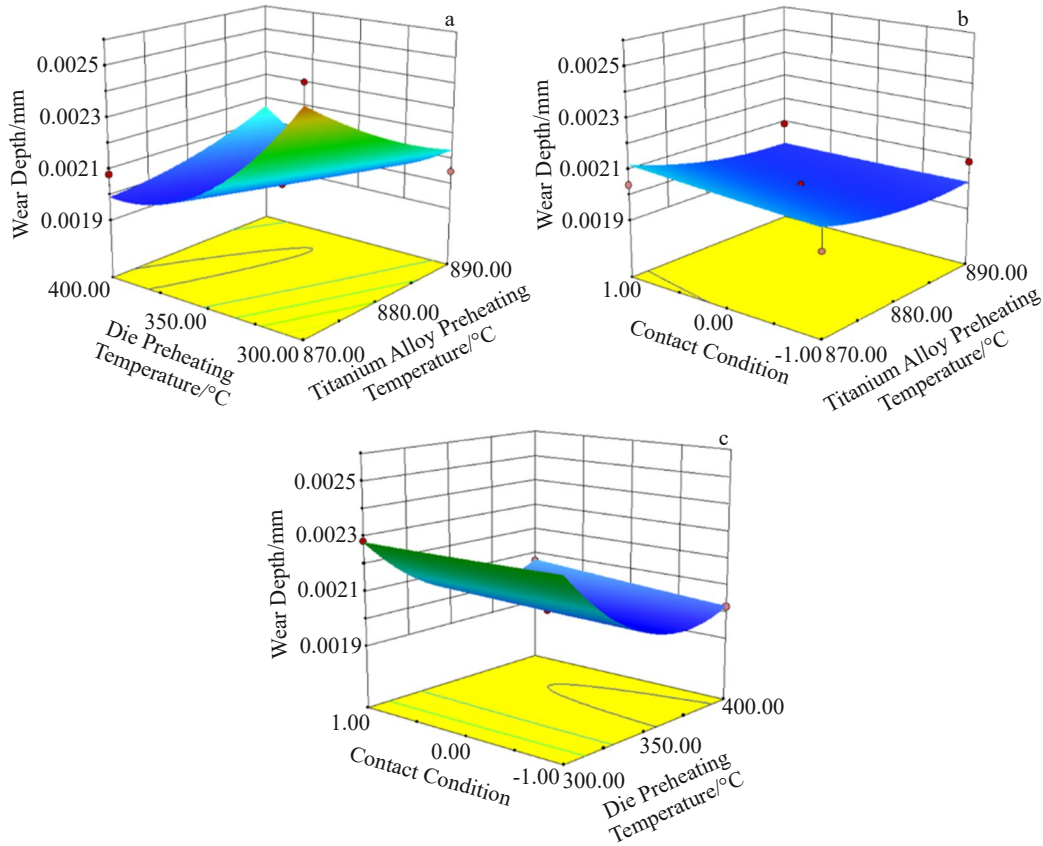
Fig.12   3D surface plots of wear depth at different conditions: (a) varying die and titanium alloy preheating temperatures, (b) varying titanium alloy preheating temperatures and contacting conditions, and (c) varying die preheating temperatures and contacting conditions

Table 9   Minimum of CDM content and wear depth in different contact conditions

Contact condition	The minimum CDM content	The minimum wear depth/mm
Bare metal	0.297	0.001 99
With glass fiber and lubricant	0.282	0.002 09
With new glass fiber	0.274	0.002 02

Table 9 shows the minimization of the CDM content and wear depth in different contact conditions. The CDM content reduces to the minimum when the wear depth is about 0.002 02 mm. The corresponding parameters are as follows: the preheating temperature of the billet is 873 °C and the die temperature is about 383 °C with new glass fiber. To prove the reliability and accuracy of optimization results, another numerical simulation of the frame forging was carried out by the optimized process parameters. The CDM content and wear depth are 0.274 and 0.002 03 mm, indicating the reliability of regression model.

3 Conclusions

1) With the aid of the secondary developed interface provided by DEFORM, the mathematical model of die wear and the CDM prediction is programmed. The experimental results of the wear and the CDM depth agree well with the simulations.

2) The response surface models can better describe objective functions of the wear depth and the CDM depth to design variables, including forging temperatures, die preheating temperatures and contact conditions, with high reliability and fitting accuracy, which can be used for subsequent multi-objective optimization.

3) The preheating temperature of die plays a dominant role in the variation of the wear depth. The most influential factor of CDM content is the contact condition. Besides, applying glass fiber can both hinder the softening of materials and decrease the wear depth even though it will aggravate the friction. Deformation heat is an essential internal factor for the two targets. The CDM content is not positively correlated with preheating temperature of die and billet.

4) The parameters can be optimized by RSM to minimize the CDM content and wear depth in TC18 frame forging process: preheating temperatures of die and billet are 383 and 873 °C, respectively, with new glass fiber.

References

1 Ning Y Q, Xie B C, Liang H Q *et al. Materials & Design*[J], 2015, 71: 68